Honda Research Institute EU
Honda Research Institute Europe GmbH
https://www.honda-ri.de/

Outdoor Particle Filter Localization with Sparse Observation

Nils Einecke, Andrej Robert

2019

Preprint:

This is an accepted article published in International Conference on Advanced Robotics. The final authenticated version is available online at: https://doi.org/10.1109/ICAR46387.2019.8981650

This article has been accepted for publication in the 2019 IEEE International Conference on Advanced Robotics.
DOI: 10.1109/ICAR46387.2019.8981650

Outdoor Particle Filter Localization with Sparse Observation

Nils Einecke[1] and Andrej Robert[2]

***Abstract*— Nowadays, autonomous lawn mowers are widely used in Europe. The robust autonomous operation and the ease of installation has lead to a substantial market share. Most autonomous lawn mowers move in a random fashion or with simple patterns because their self-localization capabilities are very limited. In this work, we analyze the potential of using apriori information about the shape of the boundary wire in combination with electromagnetic wire sensor readings for a particle-filter-based localization. In our experiments, this approach enables us to completely compensate for odometry drift. We achieve an accuracy of 20cm to 30cm in position and 3° in orientation for common garden sizes.**

I. Introduction

Vacuum cleaning and lawn mowing constitute successful applications of autonomous robots in daily life. Both have in common that they perform a quite specific task in a more or less defined area. While robotic vacuum cleaners are able to localize themselves for parallel movement, direct homing and resuming operation from the last position, most autonomous lawn mowers still miss that crucial ability. Typically, robotic vacuum cleaners use images from cameras pointing towards the ceiling for feeding SLAM algorithms [7], [9]. These algorithms have matured to a robust and accurate state for indoor navigation. Unfortunately, vision-based outdoor navigation and localization is much more challenging and research is still ongoing in particular with respect to the challenging visual changes cause by the day-night cycle or seasons [14], [17], [12].

One element that distinguishes most autonomous lawn mowers from robotic vacuum cleaners is the electromagnetic boundary wire. Robotic cleaners are physically confined by the walls and doors of the rooms they are working in. In gardens a comparable physical confinement is often not in place. Although gardens are typically surrounded by a fence, the actual lawn is usually not enclosed. Since the autonomous lawn mowers shall mow the lawn and not the flower beds, some additional means are necessary. The standard solution today is to bury a thin electric wire (boundary wire) which indicates the working area to the autonomous lawn mower with an electromagnetic field. In this work, we investigate to which extent a localization based on this electromagnetic field is possible. The appealing advantage of such an approach is that no additional hardware is required. Furthermore, the electromagnetic field generated by the wire is mostly unaffected by weather and lighting conditions in contrast to vision-based sensors.

[1]Nils Einecke is with the Honda Research Institute Europe GmbH, Carl-Legien-Strasse 30, 63073 Offenbach/Main, Germany nils.einecke@honda-ri.de

[2]Andrej Robert is with the Frankfurt University of Applied Sciences, Nibelungenplatz 1, 60318 Frankfurt/Main, Germany robert@stud.fra-uas.de

II. Related Work

Research on autonomous lawn mowers is currently a small field which is mainly concentrating on localization and object detection in this specific setting. In [22], [23] an omni-directional position estimation system for an autonomous lawn mower was introduced. The authors used an off-the-shelf robotic mower and extended it with an omni-camera and an additional compute unit. Another approach by Strisciuglio et al. [19] employs fiducial ArUco markers for localization. Unfortunately, the results on the location accuracy are rather inconclusive and the markers require substantial space.

A general problem of visual localization is the strong dependence on invariance against appearance changes on different time scales (e.g. lighting, weather, seasons) [14]. Popular local descriptors like SIFT and SURF are prone to fail in these conditions [21]. However, recently there has been increased interest to develop long-term robustness for visual localization (e.g., [12], [18], [11], [1]). Further issues when using cameras in outdoor environments on autonomous lawn mowers are artifacts caused by dirt or rain drops. It has been demonstrated that such artifacts can be detected robustly with little effort for garden robots [4]. Nevertheless, at some point an automatic cleaning procedure is inevitable making the overall system more complex and failure-prone. Finally, autonomous lawn mowers are also often programmed to work at night which is still a very challenging condition for modern visual localization techniques [16].

Franzius et al. conducted a field study on autonomous lawn mowers with visual obstacle avoidance [5]. A major insight from this study is that people are expecting more intelligence from autonomous lawn mowers in the future whether they have cameras or not. Hence, it is attractive to explore the potential of localization techniques which are not based on vision.

One example for self-localization on a lawn mower without camera is introduced in [10]. The presented system combines odometry and a gyroscope with an additional RFID system. The integration of the RFID system leads to a high accuracy and robustness as it is able to compensate for the odometry drift. On the downside, it requires extra infrastructure that needs to be installed, calibrated an maintained. A straightforward idea is to use GNSS localization (GPS, Galileo, etc.) for mower positioning. Unfortunately, GNSS localization (e.g. GPS or Galileo) does not work very well under tree canopies and near building due to blockage of

©2019 IEEE. Personal use of this material is permitted. Permission from IEEE must be obtained for all other uses, in any current or future media, including reprinting/republishing this material for advertising or promotional purposes, creating new collective works, for resale or redistribution to servers or lists, or reuse of any copyrighted component of this work in other works.

This article has been accepted for publication in the 2019 IEEE International Conference on Advanced Robotics.
DOI: 10.1109/ICAR46387.2019.8981650

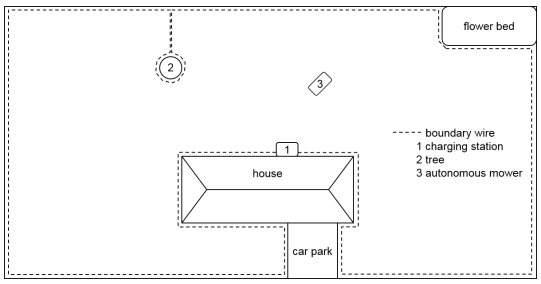

Fig. 1: Typical setup of an autonomous lawn mower with electromagnetic boundary wire.

satellite signals [13], [8]. Thus, it is not well suited for garden scenarios.

In this publication, we also target non-visual mower localization by compensating for odometry drift. Our idea is to employ the special electromagnetic boundary wire, which needs to be installed for most autonomous lawn mowers anyway. Building upon previous work [3], in which we demonstrated that the boundary wire shape can be accurately mapped with internal mower sensors (yaw sensor, wheel rate encoders, accelerometer), we utilize here the additional information about the metric shape of the wire in a particle filter framework for self-localization.

III. Boundary Wire Localization

Fig. 1 shows a typical setup of a modern autonomous lawn mower. Around the perimeter of the lawn a boundary wire is buried which is attached to a base station that acts as emitter of the electromagnetic field as well as charging station. The mower is able to perceive the presence of the field by means of hall sensors. Using the sensor readings it can measure whether it is inside or outside of the allowed area. Additionally, these sensors can be used to follow the wire, enabling the mower to find its way to the charging station. Apart from this, the basic movement of the mower is simple. It drives straight until it hits an obstacle or until it reaches the boundary wire, then it turns in a random new direction and again drives straight.

We use a particle filter framework [6], [20] for localizing an autonomous lawn mower and estimating its pose. The particle filter method is a probabilistic approach, where the estimate of the pose is represented by a probability density function (pdf). The basic idea of a particle filter is to describe the pdf by a set of N particles with corresponding weights $\{p_t^i, w_t^i\}_{i=1}^N$. The particles p^i are spread in the parameter space that is tracked according to the pdf. In our case, each particle $p_t^i = [x_t^i, y_t^i, \alpha_t^i]$ represents a hypothesis about the pose of the autonomous lawn mower at time t, where (x_t^i, y_t^i) is the position and α_t^i the orientation of the mower. Note that the height for position is omitted, since lawns are two-dimensional surfaces. The likelihood that a particle p_t^i represents the real lawnmower pose is given by the corresponding weight w_t^i. Over time, the particles are updated by two major models, a motion model and a sensor model (see Alg. III.1).

Algorithm III.1 Particle Filter Algorithm

procedure PARTICLE-FILTER($\{p_{t-1}^i\}_{i=1}^N$, u_t, z_t, ε_t^u, ε_t^z, s, $\{b^j\}_{j=1}^B$)
  for $i = 1$ to N **do**
    $p_t^i = \mathbf{motion_model}(p_{t-1}^i, u_t, \varepsilon_t^u)$
    $w_t^i = \mathbf{sensor_model}(p_t^i, z_t, \varepsilon_t^z, s, \{b^j\}_{j=1}^B)$
  end for
  for $i = 1$ to N **do**
    $w_t^i = \frac{w_t^i}{\sum_{i=1}^N w_t^i}$
  end for
  $\{p_t^i\}_{i=1}^N = \mathbf{resampling}(\{p_t^i, w_t^i\}_{i=1}^N)$
  return $\{p_t^i\}_{i=1}^N$
end procedure

The *motion model* updates the particles pose and the sensor model updates the weights. For our autonomous lawn mower scenario the motion model is the mower odometry, which is based on differential drive kinematics [2], and which can be derived from the yaw sensor and wheel rate encoder readings:

$$\begin{bmatrix}\Delta x\\ \Delta y\\ \Delta\alpha\end{bmatrix} = \begin{bmatrix}cos(\omega\Delta t) & -sin(\omega\Delta t) & 0\\ sin(\omega\Delta t) & cos(\omega\Delta t) & 0\\ 0 & 0 & 1\end{bmatrix}\begin{bmatrix}Rsin(\alpha)\\ -Rcos(\alpha)\\ 0\end{bmatrix} + \begin{bmatrix}Rsin(\alpha)\\ Rcos(\alpha)\\ \omega\Delta t\end{bmatrix}, \quad (1)$$

where

$$R = \frac{l}{2}\frac{v_r + v_l}{v_r - v_l}, \quad \text{and} \quad \omega = \frac{v_r - v_l}{l}. \quad (2)$$

In the equations above v_l and v_r represent the velocity of the left and right wheel, respectively. The distance along the axis between the wheels is l. The actual wheel velocities are calculated from the wheel rate encoder readings.

The *sensor model* realizes the knowledge gained through sensor measurements. In this work, we use the distance sensor readings from the boundary wire and base station sensors. The base station sensor output is binary. It is 1 when the mower is closer than 1m to the base station, and 0 otherwise. The boundary wire sensor provides an output based on 10 different levels whose characteristic is derived from an off-the-shelf autonomous lawn mower [15]. More formally the weights w_t^i are given by:

$$w_t^i = P(z_t^s|p_t^i) * P(z_t^b|p_t^i), \quad (3)$$

where $P(z_t^s|p_t^i)$ is the likelihood of the base station sensor measurement z_t^s given the particle pose p_t^i. Accordingly, $P(z_t^b|p_t^i)$ is the likelihood of the boundary wire sensor measurement z_t^b given the particle pose p_t^i. The sensor model for the base station is defined by:

$$P(z_t^s|p_t^i) = \begin{cases}1, & \text{if } z_t^s == z_t^{i,s}\\ 0, & \text{otherwise}\end{cases}, \quad (4)$$

where

$$z_t^{i,s} = \begin{cases}1, & \sqrt{(x_t^i - s_x)^2 + (y_t^i - s_y)^2} \le d_{max}^s\\ 0, & \text{otherwise}\end{cases}. \quad (5)$$

Here (x_t^i, y_t^i) is the particle position and (s_x, s_y) is the position of the base station. d_{max}^s is the maximal detection distance of the base station, which in our experiments is 1m.

©2019 IEEE. Personal use of this material is permitted. Permission from IEEE must be obtained for all other uses, in any current or future media, including reprinting/republishing this material for advertising or promotional purposes, creating new collective works, for resale or redistribution to servers or lists, or reuse of any copyrighted component of this work in other works.

This article has been accepted for publication in the 2019 IEEE International Conference on Advanced Robotics.
DOI: 10.1109/ICAR46387.2019.8981650

	Distance To Wire [cm]								
Wire Sensor Readings	0	10	20	30	40	50	60	70	≥ 80
4	1	0	0	0	0	0	0	0	0
5	0	1	0	0	0	0	0	0	0
6	0	0	1	0	0	0	0	0	0
7	0	0	0	0.47	0.41	0.12	0	0	0
8	0	0	0	0	0.20	0.53	0.27	0	0
9	0	0	0	0	0	0.07	0.57	0.36	0
10	0	0	0	0	0	0	0.07	0.40	0.53

TABLE I: Empiric evaluation of the in-build wire sensor readings with respect to the real metric distance to the boundary wire. The sensors output abstract distance values, as integers, ranging from 4 to 10. The table shows the likelihoods for each distance sensor value (rows) and real metric distances (columns).

The likelihood $P(z_t^b|p_t^i)$ is derived from empirical probabilities. For this, we measured the distance sensor readings and the distance to the boundary wire for about 100 different mower positions near the boundary wire [15]. As can be seen in Table I, the boundary wire sensor signal is highly correlated with the actual distance, thus constituting a very informative signal to the particle filter.

IV. Experiments

A. Setup

We analyze our novel approach by means of simulation data which we parameterized such that it is close to real data. The main problem about real data is to obtain ground truth. On the other hand, simulation is not so difficult because the move pattern of standard mowers are easy to replicate.

For the sake of reproducibility, we first generated several movement trajectories for each garden. As the trajectories are represented as position and orientation deltas it is easy to add noise with different strength afterwards and compare the particle filter performance for the same trajectory.

Fig. 2 shows the different garden shapes that we used here for testing the particle filter. All five garden shapes have been acquired from real gardens [3]. This ensures that the shapes used in the simulation have realistic properties. In particular, real garden shapes are rarely symmetric which would hamper or even break down particle filter localization due to ambiguity.

For each garden, we generated four trajectories of 5 minutes length, one trajectory of 10 minutes length and one trajectory of 60 minutes length. Each trajectory is fed several times to the particle filter in order to get enough statistics. Fig. 3 exemplarily shows the 10 minutes trajectory for each test garden. It is obvious that for larger gardens only a sub part of the area is visited and that narrow passages might lead to unvisted spaces.

The movement of autonomous lawn mowers can be described by a differential drive model [3]. Hence, the generated trajectories mainly consist of a set of position differences and angle differences for each time step. We choose a 10Hz scheme, which is reasonable high enough given the fact that autonomous lawn mowers have a maximum speed of about $1\frac{m}{s}$. For simulating sensor noise and drift, we add noise to the position and angular differences in each time step. For position noise we use $\mathcal{N}(0, 0.01m)$ and for rotation noise we use $\mathcal{N}(0, 0.1°)$. Since the mower moves 0.1m per timestep, the impact of the position noise is substantial.

B. Known Start Position

In the first set of experiments, we investigate the particle filter performance in the standard case, i.e. the mower knows its start position. Since an autonomous lawn mower will start operation most of the time from the base station, the starting position is known. Hence, it is sufficient to track the position incrementally. In order to keep comparability with later experiments we use the same random trajectories with random start positions but give the particle filter the correct position to start with. Furthermore, we differentiate between a tracking and not-tracking state of the particle filter. We define the particle filter to be in a tracking state for a time step t as follows:

$$\text{is_tracking}_t = \begin{cases} \text{error}_{\text{position}} & < & 1.5m \\ \text{error}_{\text{orientation}} & < & 25° \\ \sigma_{\text{particle_position}} & < & 2.0m \\ \sigma_{\text{particle_orientation}} & < & 10° \end{cases} \quad (6)$$

The separation between tracking and non-tracking is necessary in order to analyze the actual performance of the particle filter. In phases of non-tracking, the error is bound only by the diameter of the garden area and including those errors in the averaging of position accuracy would not lead to a meaningful insight. Instead, separating tracking and non-tracking phases enables to analyze the position accuracy of the particle filter, namely in the tracking phase. Additionally, the definition of a tracking state allows to analyze how often the particle filter looses the tracked pose and how long it takes to recover from a random initialization.

Fig. 4 depicts the position and orientation estimation result for 5, 10 and 60 minutes random trajectories for all test gardens. The results show that the position error increases with garden area size (see Fig. 2 for garden size). This is mainly caused by the missing wire sensor data when the mower is more than 1m away from the boundary wire. In these situations, the particles will spread and the estimation uncertainty increases as the mower has to rely on odometry sensor readings only. In larger gardens the non-sensor-data areas increase, so does the position error. Interestingly, the orientation error is almost unaffected. The reason is the much lower sensor noise of the yaw sensor compared to the wheel odometry, i.e. the orientation can be accurately updated over

©2019 IEEE. Personal use of this material is permitted. Permission from IEEE must be obtained for all other uses, in any current or future media, including reprinting/republishing this material for advertising or promotional purposes, creating new collective works, for resale or redistribution to servers or lists, or reuse of any copyrighted component of this work in other works.

This article has been accepted for publication in the 2019 IEEE International Conference on Advanced Robotics.
DOI: 10.1109/ICAR46387.2019.8981650

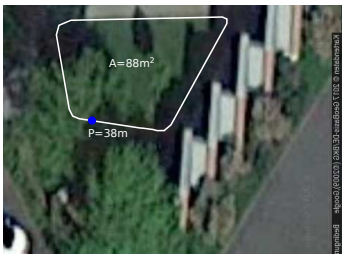

(a) Garden A

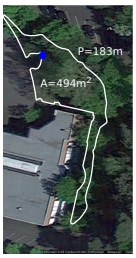

(b) Garden B



(c) Garden C

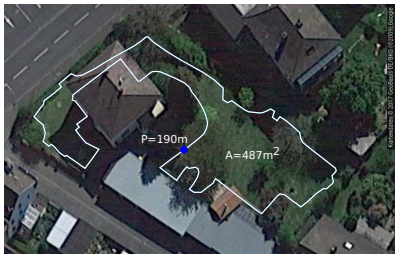

(d) Garden D

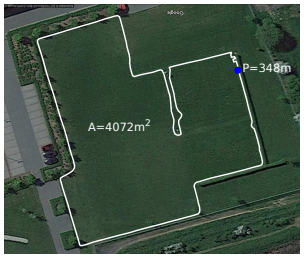

(e) Garden E

Fig. 2: These five shapes, acquired from real lawn and gardens, are used as the basis for conducting the particle filter localization experiments. We choose gardens with a wide variety of area A and the perimeter length P. The blue dot indicates the position of the base station for charging.

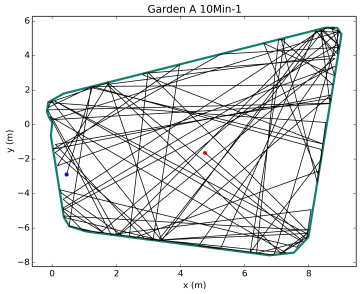

(a) Garden A

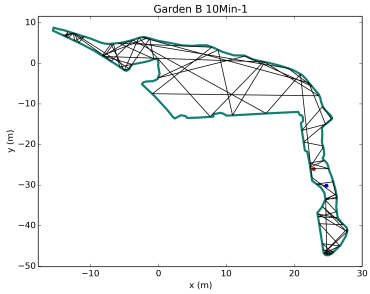

(b) Garden B

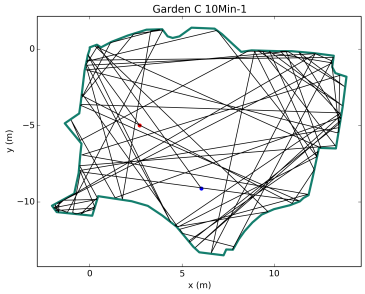

(c) Garden C

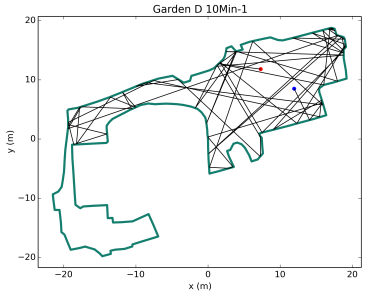

(d) Garden D

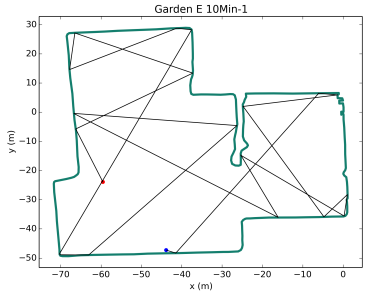

(e) Garden E

Fig. 3: Example of the simulated 10 minutes trajectories for each test garden. The blue and red dots are the starting and end positions, respectively.

longer distances without the absolute reference from the wire.

It can also be seen that the error is similar for different track lengths, which was expected, since the particle filter has access to the start position. However, it also highlights that the particle filter is able to keep track of the mower movements and does not loose the pose. Moreover, it demonstrates that for the standard autonomous mower scenario a particle filter can track the mower pose within the garden with and accuracy of 0.2m to 0.6m and about 3°. The achieved accuracy enables many important features such as direct homing, zone mowing or coverage estimation.

©2019 IEEE. Personal use of this material is permitted. Permission from IEEE must be obtained for all other uses, in any current or future media, including reprinting/republishing this material for advertising or promotional purposes, creating new collective works, for resale or redistribution to servers or lists, or reuse of any copyrighted component of this work in other works.

This article has been accepted for publication in the 2019 IEEE International Conference on Advanced Robotics.
DOI: 10.1109/ICAR46387.2019.8981650

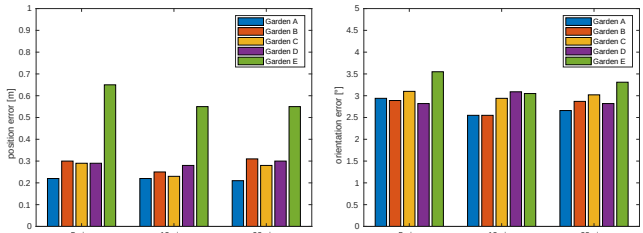

(a) Position Error (b) Orientation Error

Fig. 4: This plot shows the average position and orientation estimation error of the particle filter for the different gardens A-E. Here, the particle filter was initialized with a known start position.

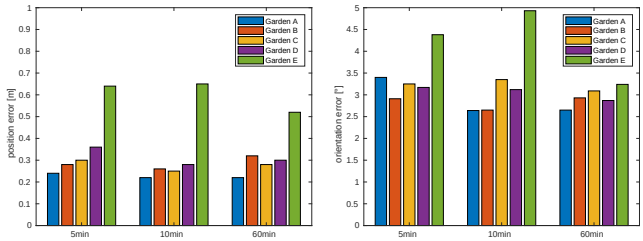

(a) Position Error (b) Orientation Error

Fig. 5: This plot shows the average position and orientation estimation error of the particle filter for the different gardens A-E. Here, the particle filter had no information on the start position.

However, mowing patterns such as parallel lanes require an accuracy of less than 0.1m. Please note, that the relatively low accuracy of 0.6m is achieved only on the largest garden. For all other gardens, the approach achieves a substantially higher accuracy of 0.2-0.3m.

C. Unknown Start Position

For the next experiment, the particle filter had no access to the starting position, but instead it had to bootstrap itself. Naturally, such a task is more challenging. We use exactly the same trajectories as in the experiment (last section IV-B) with the known start position. This enables us to compare the two results.

Fig. 5 shows the average position and orientation errors when the particle filter is in tracking state, i.e. has already found the mower pose. The results are quite similar to those achieved with access to the starting position. However, the average orientation error for the 5 and 10 minutes tracks are higher than in the known start position experiments. We think that in this case the particle filter already follows the pose with less accurate orientation estimations. Probably, this depends on the time between two boundary wire events, as the particle filter can only correct for errors when measuring the boundary wire signal. This explanation is further supported by the slightly higher position error for the largest garden E where the boundary wire is measured less frequently.

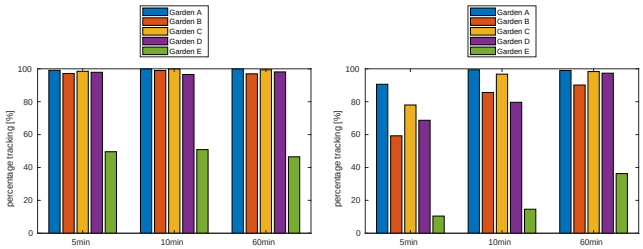

(a) Start Position Known (b) Start Position Unknown

Fig. 6: This plot shows what percent of the time the particle filter is correctly tracking the position of the lawn mower according to our definition.

The results in Fig. 5 highlight that the pose estimation performance of the particle filter is similar for both correct pose initialization and unknown start pose once it has reached a tracking state. In this regard, a key question is: *How long does it take until the particle filter is able to track the position?* In order to shed some light on this question, Fig. 6 depicts the percentage of time the particle filter is in tracking state for 5, 10 and 60 tracks for both known and unknown start pose experiments. The bar plots show that for the known start pose the tracking time percentage is almost the same for 5, 10 and 60 minutes tracks. In contrary, the tracking time increases with trajectory length for unknown start poses, since the particle filter requires some time to resolve the mower pose. Moreover, the tracking time is higher for smaller gardens due to a quicker determination of the mower pose. For the small gardens A and C the pose is already resolved after 5 minutes. In case of the average sized gardens B and D, it takes about 10 minutes, whereas, the pose resolving in the largest garden E requires more than 10 minutes. It has to be noted, however, that the tracking time measurement we defined above does not work so well for garden E. Even in the case of known start pose the tracking time was only about 50% for 5, 10 and 60 minutes tracks. The problem is the strong particle spread when driving long straights through the garden without hitting a boundary wire for correction measurements.

To provide a more detailed analysis of the tracking performance, Fig. 7 depicts the position and orientation error over the course of 60 minutes track in garden E. The plots are colored over time. Times where the mower does not sense any wire nearby are colored greenish, times where the mower is able to measure a distance to the wire are colored blueish. As the plots Fig. 7a and Fig. 7b show, the random particle initialization leads to a high error in position and orientation at the beginning. It takes about 14 minutes until the particle filter has converged to the correct mower pose. During this convergence phase the error ranges between 15m and 70m and up to up to $180°$ for position and orientation, respectively. After the initial convergence the error intermediately can still rise to 20m and $25°$ but is brought down to almost zero at each visit of the boundary wire. To get a better view on this Fig. 7c depicts a cutout

©2019 IEEE. Personal use of this material is permitted. Permission from IEEE must be obtained for all other uses, in any current or future media, including reprinting/republishing this material for advertising or promotional purposes, creating new collective works, for resale or redistribution to servers or lists, or reuse of any copyrighted component of this work in other works.

This article has been accepted for publication in the 2019 IEEE International Conference on Advanced Robotics.
DOI: 10.1109/ICAR46387.2019.8981650

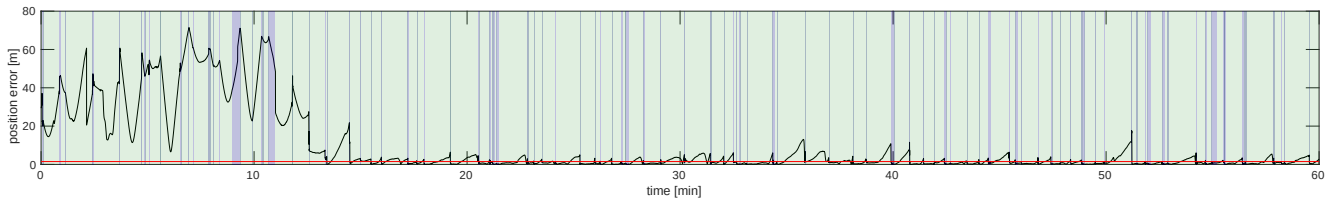

(a) Position Error

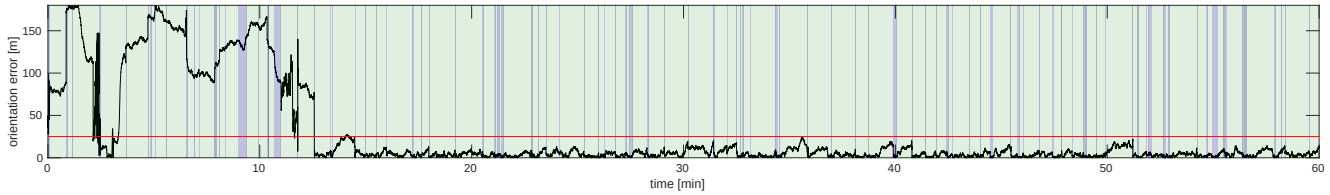

(b) Orientation Error

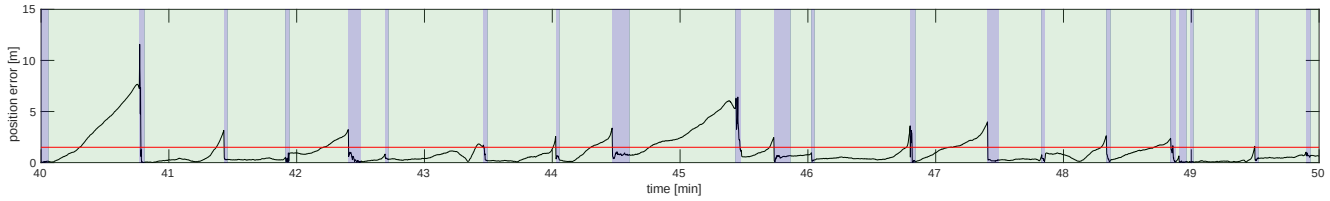

(c) Position Error Cutout Minute 40-50

Fig. 7: These plots shows the position and orientation error of the particle filter over the course of a 60 minutes trajectory in the large garden E. The blue color encodes times where the mower is able to perceive the boundary wire, whereas the green color marks times where the signal is unavailable (mower is in the middle of the garden). The red line represents the threshold of 1.5m and 25° where we consider the particle filter to track the correct pose.

of the position error ranging from minute 40 to 50. This plot nicely visualizes the increase in position error caused by the increase in uncertainty over time when no boundary or base station measurements are available. During these times (greenish coloring) the particle filter can only perform the particle pose update without adapting the weights. Hence, the particle cloud starts to diverge and consequently the estimated mower pose. As soon as the mower comes into sensing range for the boundary wire (blueish coloring) the weights are updated, leading to a quick reduction of the accumulated error. This phenomena causes the resulting heartbeat-like pattern of the position error plotted over time.

In order to get an idea how often an autonomous lawn mower visits the boundary wire during operation hours Table II lists various statistics for gardens A to E. The most important value is the boundary wire ratio, which is the percentage of time the mower is able to perceive the boundary wire by measuring a distance to it with its electromagnetic field sensors. As it can be seen, this is only the case for a small fraction of the overall time. Consequently, the particle filter has only a very limited amount of time to correct the pose estimation. For a more detailed view, the table also lists the number wire events (boundary wire encounters) and the number of base station visits (only detection, not going in for charging). Obviously, the number of base station visits decreases with the garden area. For the large garden E, the base station was encountered only once during the 60 minute trajectory. The number of wire events is indirectly linked to the garden size as it also depends on the specific shape. The number of wire visits correlate with the perimeter-area ration, i.e. the ratio between boundary wire length and garden area.

D. Remaining Issues

During our experiments, we encountered several problems which remained unsolved but are crucial in order to develop the technology further.

First, the efficiency for computing the weight updates needs to be improved. The boundary wire is represented as a polyline. Thus, it is necessary to compute the distance of each particle to each line segment which leads to a runtime complexity of $\mathcal{O}(p*s)$, where p is the number of particles and s is the number of line segments. To put it more concretely, for 2000 particles and 100 line segments it is necessary to compute 2 million point-lines distances.

Second, we get some additional error by the way we compute the estimated mower position. For computing the estimated pose we simply average over all particles. This works well except when the mower comes close the the wire. In these cases particles too close to the boundary will be deleted due to low importance weights which causes a deformation of the particle cloud. A corresponding example is depicted in Fig. 8. While the mower is still in the center garden area, the particle cloud distributes in a Gaussian shape around the real position (Fig. 8a). As soon as the mower comes close to the wire, particles moving too far into the direction of the wire will be deleted due to a low number of

©2019 IEEE. Personal use of this material is permitted. Permission from IEEE must be obtained for all other uses, in any current or future media, including reprinting/republishing this material for advertising or promotional purposes, creating new collective works, for resale or redistribution to servers or lists, or reuse of any copyrighted component of this work in other works.

This article has been accepted for publication in the 2019 IEEE International Conference on Advanced Robotics.
DOI: 10.1109/ICAR46387.2019.8981650

TABLE II: This table summarized statistics about base station and boundary wire visits of the autonomous lawn mower during operation.

	Garden A	Garden B	Garden C	Garden D	Garden E
boundary wire time ratio	3.82%	2.93%	2.81%	2.81%	0.99%
wire events per hour	396	343	340	326	102
base events per hour	48	7	20	9	1
garden area m^2	88	494	158	487	4072
garden perimeter m	38	183	56	190	348
perimeter-area ratio	0.43	0.37	0.35	0.39	0.09

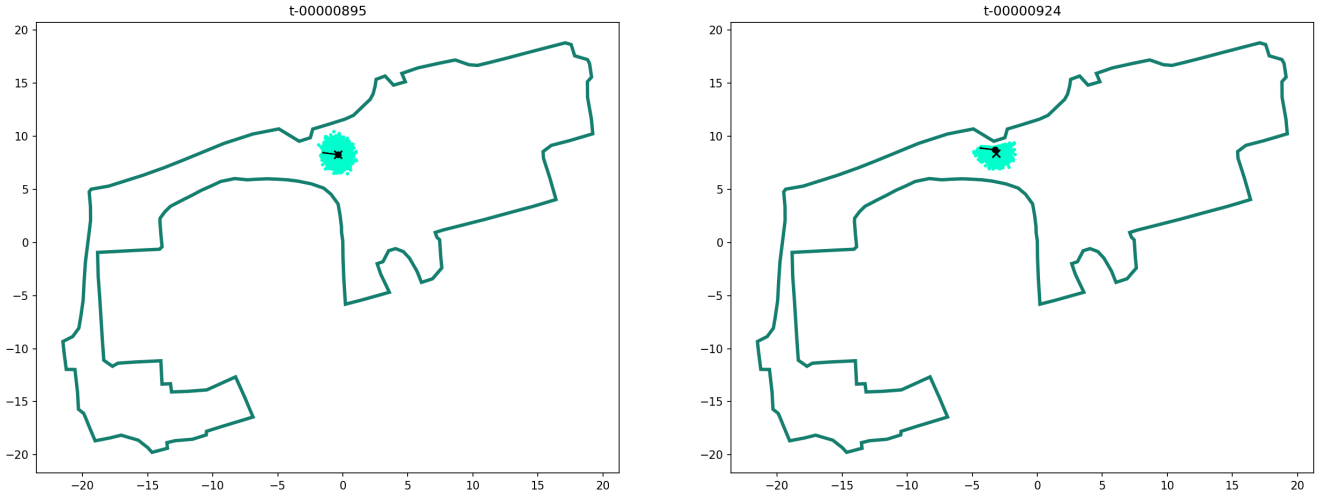

(a) Infield (b) Close to Wire

Fig. 8: These images highlight the particle cloud deformation problem that occurs near the boundary wire. The dot and the arrow indicated real mower position and orientation, respectively. The cross indicates the average particle position. The particle cloud deformation leads to position estimation errors.

importance weights. Since the actual mower position is not in boundary wire measurement range, particles that have a position in measurement range get a low importance weight as the electromagnetic field sensor readings do not support such a close position. This leads to a strong deformation of the particle cloud (see Fig. 8b) which in turn leads to wrong position estimates. One way to tackle the cloud deformation problem is to reduce the particle divergence. This can be done by a parameter optimization, which needs to be addressed and investigated in future work.

Third, the particle filter needs to be evaluated on real mower data. Unfortunately, the ground truth pose measurement for autonomous lawn mowers is largely unsolved. (Differential) GPS does not work well due to the abundance of sky occlusion in many gardens and marker based tacking becomes quickly unfeasible for larger gardens.

Fourth, the particle filter implementation is missing a self-assessment for the tracking state. Currently, we only do this offline by using the ground truth position. Unfortunately, basing this only on particle spread does not work and we need to research alternatives in future work.

V. Conclusion

In this work, we tackled the pose estimation for autonomous lawn mowers moving in an area constrained by an electromagnetic boundary wire. We applied and analyzed an approach based on the standard particle filter. The main idea is to use the metric shape of the boundary wire as map data for our particle filter. Since the map consists only of the wire, it is very sparse and the particle filter is only able to infer or refine the mower pose when the mower is close to the boundary wire and distance measures to the wire are available.

Due to a lack of ground truth acquisition in real gardens, we performed a series of experiments in simulation. The simulated data, however, is based on real garden boundary wire shapes and, thus, captures at least real garden characteristics. The experiments demonstrate that localization using off-the-shelf autonomous lawn mowers has an average accuracy of 0.2m to 0.3m in position and 3° in orientation for common garden sizes. For larger gardens the error increases to 0.6m in position. We showed that our particle filter framework is able to localize the mower starting from an unknown start position. This worked for all test gardens which range from $88m^2$ up to $4072m^2$ in size.

In future work, we would like to tackle the computational complexity. Currently, the approach is inefficient since it computes point-line distances for every particle and every boundary segment. Furthermore, we would like to test our

©2019 IEEE. Personal use of this material is permitted. Permission from IEEE must be obtained for all other uses, in any current or future media, including reprinting/republishing this material for advertising or promotional purposes, creating new collective works, for resale or redistribution to servers or lists, or reuse of any copyrighted component of this work in other works.

This article has been accepted for publication in the 2019 IEEE International Conference on Advanced Robotics.
DOI: 10.1109/ICAR46387.2019.8981650

system on real mower data. The main challenge here is to acquire ground truth position and orientation data because differential GPS is often unavailable within gardens. Eventually, we target to bring our particle filter onto a real lawn mower running in real-time on close-to-production embedded hardware.

REFERENCES

[1] W. Churchill and P. Newman. Experience-based navigation for long-term localisation. *The International Journal of Robotics Research*, 32(14):1645–1661, 2013.

[2] G. Dudek and M. Jenkin. *Computational principles of mobile robotics*. Cambridge university press, 2010.

[3] N. Einecke, J. Deigmöller, K. Muro, and M. Franzius. Boundary wire mapping on autonomous lawn mowers. In *International Conference on Field and Service Robotics (FSR)*, pages 351–365, 2017.

[4] N. Einecke, H. Gandhi, and J. Deigmöller. Detection of camera artifacts from camera images. In *17th International IEEE Conference on Intelligent Transportation Systems (ITSC)*, pages 603–610, 2014.

[5] M. Franzius, M. Dunn, N. Einecke, and R. Dirnberger. Embedded robust visual obstacle detection on autonomous lawn mowers. In *Conference on Computer Vision and Pattern Recognition Workshops*, pages 361–369, 2017.

[6] N. J. Gordon, D. J. Salmond, and A. F. M. Smith. Novel approach to nonlinear/non-gaussian bayesian state estimation. *IEE Proceedings F - Radar and Signal Processing*, 140(2):107–113, 1993.

[7] H.-K. Lee, K. Choi, J. Park, and H. Myung. Self-calibration of gyro using monocular SLAM for an indoor mobile robot. *International Journal of Control, Automation and Systems*, 10(3):558–566, 2012.

[8] I.-S. Lee and L. Ge. The performance of rtk-gps for surveying under challenging environmental conditions. *Earth, Planets and Space*, 58(5):515–522, 2006.

[9] S. Lee, S. Lee, and S. Baek. Vision-based kidnap recovery with SLAM for home cleaning robots. *Journal of Intelligent & Robotic Systems*, 67(1):7–24, 2012.

[10] A. Levratti, C. Secchi, and C. Fantuzzi. A low cost localization algorithm for an autonomous lawnmower. In *Robot Motion and Control (RoMoCo), 2013 9th Workshop on*, pages 276–281. IEEE, 2013.

[11] B. Metka, A. Besetzny, U. Bauer-Wersing, and M. Franzius. Predicting the long-term robustness of visual features. In *International Conference on Advanced Robotics (ICAR)*, pages 465–470. IEEE, 2015.

[12] T. Naseer, W. Burgard, and C. Stachniss. Robust visual localization across seasons. *IEEE Transactions on Robotics*, 34(2):289–302, 2018.

[13] R. B. Ong, M. G. Petovello, and G. Lachapelle. Assessment of gps/glonass rtk under various operational conditions. In *Proceedings ION GNSS*, pages 3297–3308, 2009.

[14] N. Piasco, D. Sidibé, C. Demonceaux, and V. Gouet-Brunet. A survey on visual-based localization: On the benefit of heterogeneous data. *Pattern Recognition*, 74:90–109, 2018.

[15] A. Robert. Mobile robot self-localization based on particle filter and boundary shape information. Master's thesis, Frankfurt University of Applied Sciences, 2018.

[16] T. Sattler, W. Maddern, C. Toft, A. Torii, L. Hammarstrand, E. Stenborg, D. Safari, M. Okutomi, M. Pollefeys, J. Sivic, F. Kahl, and T. Pajdla. Benchmarking 6dof outdoor visual localization in changing conditions. In *The IEEE Conference on Computer Vision and Pattern Recognition (CVPR)*, 2018.

[17] J. L. Schönberger, M. Pollefeys, A. Geiger, and T. Sattler. Semantic visual localization. In *The IEEE Conference on Computer Vision and Pattern Recognition (CVPR)*, pages 6896–6906, 2018.

[18] T. Stone, D. Differt, M. Milford, and B. Webb. Skyline-based localisation for aggressively manoeuvring robots using UV sensors and spherical harmonics. In *IEEE International Conference on Robotics and Automation (ICRA)*, pages 5615–5622. IEEE, 2016.

[19] N. Strisciuglio, M. L. Vallina, N. Petkov, and R. M. Salinas. Camera localization in outdoor garden environments using artificial landmarks. In *2018 IEEE International Work Conference on Bioinspired Intelligence (IWOBI)*, pages 1–6, 2018.

[20] S. Thrun, W. Burgard, and D. Fox. *Probabilistic Robotics (Intelligent Robotics and Autonomous Agents)*. The MIT Press, 2005.

[21] C. Valgren and A. J. Lilienthal. SIFT, SURF & seasons: Appearance-based long-term localization in outdoor environments. *Robotics and Autonomous Systems*, 58(2):149–156, 2010.

[22] J. Yang, S.-J. Chung, S. Hutchinson, D. Johnson, and M. Kise. Vision-based localization and mapping for an autonomous mower. In *IEEE/RSJ International Conference on Intelligent Robots and Systems (IROS)*, pages 3655–3662, 2013.

[23] J. Yang, S.-J. Chung, S. Hutchinson, D. Johnson, and M. Kise. Omnidirectional-vision-based estimation for containment detection of a robotic mower. In *IEEE International Conference on Robotics and Automation (ICRA)*, pages 6344–6351, 2015.

©2019 IEEE. Personal use of this material is permitted. Permission from IEEE must be obtained for all other uses, in any current or future media, including reprinting/republishing this material for advertising or promotional purposes, creating new collective works, for resale or redistribution to servers or lists, or reuse of any copyrighted component of this work in other works.